Optical Processing Based on Spectral Line-by-Line Pulse Shaping on a Phase-Modulated CW Laser

Zhi Jiang, *Student Member, IEEE*, Daniel E. Leaird, *Senior Member, IEEE*, and Andrew M. Weiner, *Fellow, IEEE*

***Abstract*—We demonstrate optical processing based on spectral line-by-line pulse shaping of a frequency comb generated by phase modulating a CW laser and show various applications including CW-to-pulse conversion, width/wavelength tunable return-to-zero pulse generation, pulse-to-CW conversion, wavelength conversion, and microwave photonics. The correlations between optical spectra, time-domain waveforms, and RF spectra are quantitatively studied.**

***Index Terms*—Line-by-line pulse shaping, optical processing, phase modulator.**

I. Introduction

PERIODIC pulses are characterized in the frequency domain by an evenly spaced series of discrete spectral lines (optical frequency comb), with the frequency spacing equal to the pulse repetition rate. Pulse-shaping techniques, in which intensity and phase manipulation of optical spectral components allow synthesis of user-specified pulse fields according to a Fourier transform relationship, have been developed and widely adopted [1]. Past pulse shapers have generally manipulated groups of spectral lines rather than individual lines, which results in waveform bursts that are separated in time with low duty factor and which are insensitive to the absolute frequency positions of the mode-locked comb. This is primarily due to the practical difficulty of building a pulse shaper that is capable of resolving each spectral line for typical mode-locked lasers with repetition rates below 1 GHz. With the possibility to extend pulse shaping to independently manipulate the intensity and phase of individual spectral lines (i.e., line-by-line pulse shaping), the shaped pulses can overlap with each other, which leads to waveforms spanning the full time period between mode-locked pulses (100% duty factor). Waveform contributions arising from adjacent mode-locked pulses will overlap and interfere coherently in a manner sensitive to the offset of the frequency comb [2]. Such line-by-line control is an important step towards optical arbitrary waveform generation (O-AWG), since the intensity and phase of each individual spectral line is independently controlled. Previous efforts towards spectral line-by-line control utilized a hyperfine filter but were limited within a narrow optical bandwidth—the free spectral range of this device [3], [4]. Recently, we demonstrated spectral intensity/phase line-by-line pulse shaping [2] and, thus, O-AWG over a considerably broader band [5] based on high-resolution grating-based pulse shapers.

In prior demonstrations, the spectral lines (or periodic pulses) are generated by high-repetition-rate mode-locked lasers. Such spectral lines can suffer from instability problems [2], which hinders the development of the line-by-line pulse-shaping technique. An alternative technique to generate a well-defined comb of spectral lines is applying strong periodic modulation on a CW laser [6]–[13]. This is an old idea [6], and results generating combs spanning multiple THz have been obtained using high-power microwave drives [7], [8]. Some simple optical processing functionalities have been recently demonstrated based on a modulated CW laser. For example, a modulated CW laser is followed by single-mode fiber or other dispersion components for pulse generation [9]–[11], followed by an array waveguide grating for wavelength conversion [12] and followed by a fiber Bragg grating for microwave photonics applications [13]. However, the demonstrated functions are largely limited by these simple processing devices which have very limited and fixed (i.e., nontunable) capabilities. In this study, we demonstrate spectral line-by-line pulse shaping on a modulated CW laser, which significantly extends the capability of optical processing with a modulated CW laser, since the intensity/phase of all individual spectral lines can be independently and programmably controlled. The bandwidth of spectral lines generated by a modulated CW laser is especially suitable to optical fiber communication applications, some of which will be shown below.

Compared with the spectral comb generated from a mode-locked laser, the comb from a modulated CW laser possesses the following advantages: lower cost and lower complexity, simple tuning of the comb offset frequency (spectral line position), continuous tunability of the spectral line separation (the repetition rate), and reasonably stable operation without active control. Although highly stable and tunable mode-locked lasers are available now, for example, Ti:Sapphire lasers built with the state-of-the-art technique [14], the repetition rates are usually limited to around 1 GHz for such stabilized lasers. Our current line-by-line pulse-shaping technique requires higher repetition rates in order to cleanly resolve lines; such higher rates are also more interesting for optical communication applications. However, at high repetition rates, frequency-stabilized lasers have been demonstrated only with very complicated control and with tunability significantly compromised [15]. Furthermore, this "modulation-of-CW" scheme has the significant advantage that frequency offset and coherence of individual lines are controlled by the input CW laser and are decoupled from the pulse

Manuscript received March 3, 2006; revised April 11, 2006. This work was supported by the Defense Advanced Research Projects Agency (DARPA) under Grant MDA972-03-1-0014 and by the Air Force Office of Scientific Research/DARPA under Grant FA9550-06-1-0189.

The authors are with the School of Electrical and Computer Engineering, Purdue University, West Lafayette, IN 47907-2035 USA (e-mail: zjiang@purdue.edu; leaird@purdue.edu; amw@ecn.purdue.edu).

Digital Object Identifier 10.1109/JQE.2006.876716

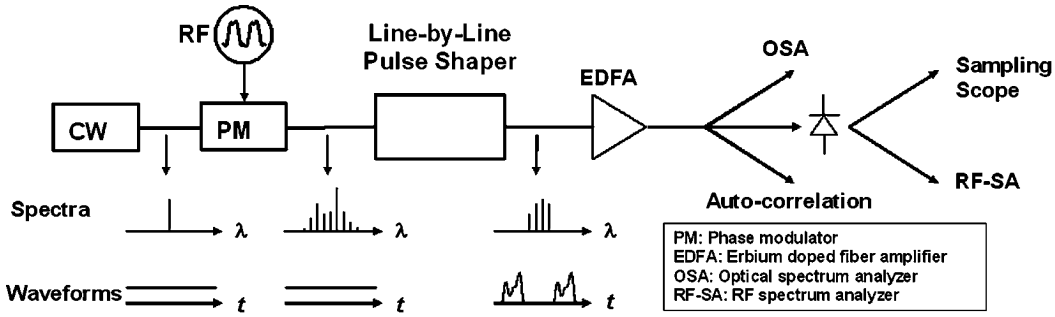

Fig. 1. Experimental setup.

generation process; this provides a degree of control that is not yet readily available at high (e.g., 2.5–10 GHz) repetition rates from mode-locked sources. A drawback is that timing jitter is, in principle, impacted by the driving electronics (as indeed is the case for harmonically mode-locked lasers). However, this had no observable effect in the experiments reported here.

In addition to the applications for optical processing, since we are able to gain control over the comb using a CW modulation scheme, it lets us study the new fundamental issues in line-by-line shaping. This will elucidate issues that will also be important when pulse shaping is used with true stabilized combs. In particular, we present here a multiple-spectral-lines-to-single-spectral-line (i.e., comb-to-CW) conversion experiment and investigate the correlation between the optical spectrum, the electrical spectrum, and the time-domain waveforms as the suppression ratio of undesired lines is intentionally compromised. Frequency-comb-to-single-frequency conversion is perhaps the simplest operation possible in line-by-line shaping; our experiments examining the effect of imperfect suppression of undesired lines adds insight into what is required for good waveform fidelity in line-by-line shaping.

II. Experiments and Discussions

A. Experimental Setup

Fig. 1 shows our experimental setup. A tunable CW laser (Agilent 8163A, with linewidth ~60 MHz) is modulated by a phase modulator, which is driven by the clock signal from a bit-error-rate (BER) test set. The generated spectral lines are then manipulated by the spectral line-by-line pulse shaper. The resulting optical signal is measured by an optical spectrum analyzer (OSA) with 0.01-nm resolution and intensity autocorrelation measurement apparatus. The output signal is also detected by a 50-GHz photodiode and measured by an RF spectrum analyzer (0–50 GHz) and sampling scope with 50-GHz bandwidth. The phase modulator has a V_π of ~ 5 V. As an alternative, an intensity modulator can also be used for the purpose of spectral comb generation.

Fig. 2 shows the experimental setup of a line-by-line pulse shaper, in which a fiber coupled Fourier-transform pulse shaper is constructed in a reflective geometry. A fiber-pigtailed collimator and subsequent telescope take the light out of fiber and magnify the beam size to ~ 18 mm diameter on the 1200-grooves/mm grating in order to enhance the pulse-shaper resolution. Discrete spectral lines making up the input short

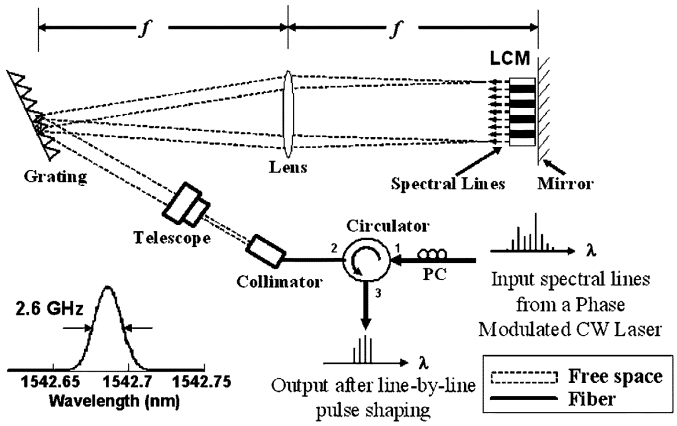

Fig. 2. Line-by-line pulse shaper. The inset figure shows a measured 3-dB passband of 2.6 GHz. LCM: liquid crystal modulator. PC: polarization controller.

pulse are diffracted by the grating and focused by the lens with 1000-mm focal length. A fiberized polarization controller (PC) is used to adjust for horizontal polarization on the grating. A 2×128 pixel liquid crystal modulator (LCM) array with a polarizer on the input face is placed just before the lens focal plane to independently control both amplitude and phase of individual spectral lines. The individual pixels of the LCM, arranged on 100-μm centers, can be electronically controlled independently to give amplitude and phase control. A retro-reflecting mirror leads to a double-pass geometry, with all of the spectral lines recombined into a single fiber and separated from the input via an optical circulator. The fiber-to-fiber insertion loss is 11.6 dB (including circulator loss), which includes all optical component losses as well as loss incurred in focusing back into the 9-μm fiber mode after the pulse shaper. The loss in the system is compensated by an erbium-doped fiber amplifier. The passband width, which is measured by scanning a tunable, narrow-linewidth, CW laser with the LCM replaced by a narrow slit, is 2.6 GHz at the 3-dB points, as is shown in the inset. The passband is mainly caused by the finite spot size at the LCM plane, which is affected by the pulse-shaper design [1]. The high resolution makes accurate and independent control of individual spectral lines possible and enables line-by-line pulse-shaping control, potentially over a broad optical band.

B. Generation and Control of Spectral Lines

Fig. 3(a) shows the optical spectrum of the CW laser, which is characterized as a single spectral line. Fig. 3(b) shows the gen-

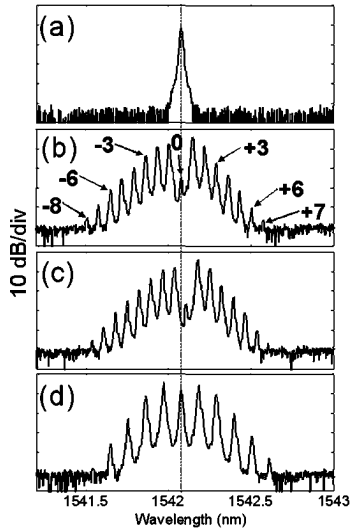

Fig. 3. Spectra of: (a) input CW and (b) phase-modulated CW at 9.0 GHz, (c) phase-modulated CW at 9.0 GHz but tuning the input CW wavelength, and (d) phase-modulated CW at 13.5 GHz.

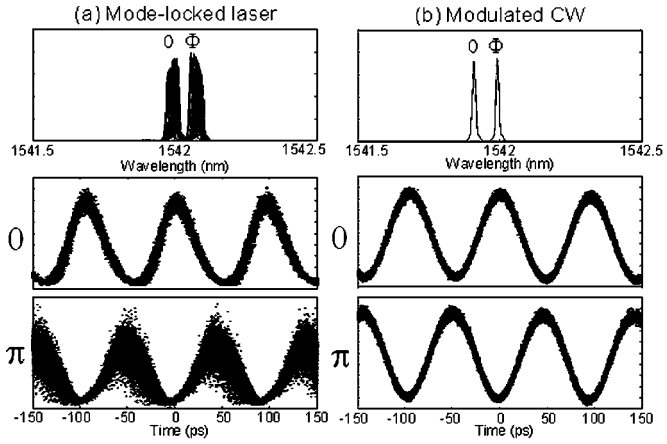

Fig. 4. (a) Unstable spectral lines and corresponding waveforms from an actively mode-locked fiber laser running at 10.5 GHz. Noise process is observed when applying π phase shift on one of the two lines. (b) Stable spectral lines and corresponding waveforms from a modulated CW at 10.5 GHz. No such noise process is observed.

erated optical spectral lines after the phase modulator driven by a 9.0-GHz clock signal. Even though our current phase modulator limits us to only $\sim 1.6\pi$ phase shift, a total of 16 comb lines are visible above the noise floor of our measurement with this phase shift, covering a bandwidth of 135 GHz. Such a bandwidth is particularly useful for optical fiber communications and microwave photonics applications. The bandwidth could be significantly enhanced by applying higher RF power, lowering modulator V_π, cascading modulators, and using a phase modulator with optical resonance configuration [8]. The asymmetry of the spectral lines is caused by the nonpure cosine driving RF signal, which has little impact on our demonstration since the intensity of individual lines can be controlled. Fig. 3(c) confirms that tuning the frequency of the source laser results in a corresponding shift of the generated comb, demonstrating controllability of the spectral line positions or the offset of frequency comb. This offset of frequency comb and its control in the mode-locked laser play a critical role in recent advances in optical metrology [16], [17]. The results shown here provide an alternative way to control it. Fig. 3(d) shows the spectral lines with a 13.5-GHz driving signal (with similar bandwidth), demonstrating controllability of the spectral line separations.

C. Spectral-Line Fluctuation and its Impact on Line-by-Line Pulse Shaping

Intuitively, full control of individual spectral lines requires frequency-stabilized sources to generate stable spectral lines in addition to the high-resolution pulse shapers to resolve and control individual spectral lines. To illustrate this point, in this section, we compare the results of pulse shaping on a relatively unstable mode-locked laser and the phase-modulated CW laser. For this purpose, two spectral lines are selected by the pulse shaper and the corresponding cosine waveforms in the time domain are studied. Fig. 4 shows the relationship between spectral line stability and waveform noise process. Fig. 4(a) shows an overlap of multiple scans for the two spectral lines and sampling scope traces from our harmonically mode-locked fiber laser running at 10.5 GHz, which shows observable frequency fluctuations. The cosine waveform is relatively clean if no phase shift is applied. However, if π phase shift is applied on one of the spectral lines, the waveform shows a strong noise effect. As clarified in [2], the noise occurs due to the effect of fluctuations in the pulse-to-pulse phase on the interference of shaped waveform contributions arising from two different mode-locked pulses. Note that the behaviors of spectral-line fluctuations highly depend on the characteristics of the particular mode-locked laser. In contrast, the phase-modulated CW at 10.5 GHz in Fig. 4(b) shows spectral lines with reasonably good stability. The waveforms are clean for both 0 and π phase shift on one of the two spectra lines. The CW source used in our experiments has a $\sim$ 60-MHz fluctuation, which is sufficiently stable to allow clear demonstration of various optical processing functionalities using line-by-line pulse shaping, as we report later in this paper. The simple comparison study in Fig. 4 shows the importance to have stable spectral lines for line-by-line pulse shaping. The approach of a phase-modulated CW laser provides a simple and flexible solution for generating spectral lines with reasonably good stability.

D. CW-to-Pulse Conversion

Hereafter, we show various optical processing functionalities based on spectral line-by-line pulse shaping on a phase-modulated CW laser, in which spectral lines with 9.0-GHz separation as shown in Fig. 3(b) are used unless otherwise specified. Fig. 5(a) shows the time-domain waveform corresponding to Fig. 3(b) as measured by a sampling scope. The phase-modulated waveform remains at almost a constant intensity, as is expected, since only the temporal phase is modulated. From now on, we use the line-by-line pulse shaper to manipulate the spectral lines of the modulated CW laser to show optical processing capabilities. The LCM pixel spacing is matched to the 9.0-GHz spectral-line spacing (each line is controlled by every two pixels) by setting an appropriate grating diffraction angle. By correcting the spectral phase of the individual lines using the

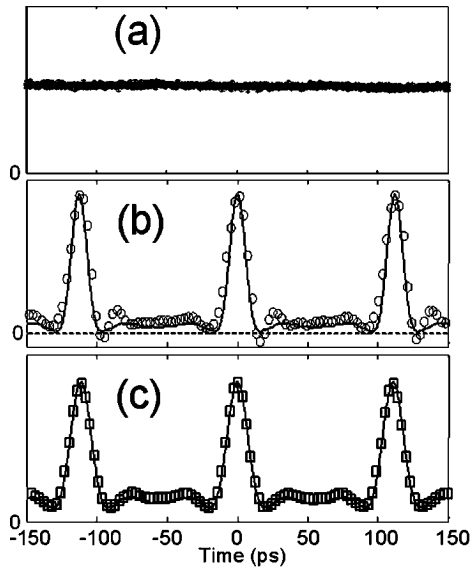

Fig. 5. CW-to-pulse conversion. (a) Sampling scope trace of phase-modulated CW. (b) Pulses measured via sampling scope after spectral phase correction (circles) and calculation (solid line). (c) Measured (squares) and calculated (solid line) pulse intensity autocorrelation.

line-by-line pulse shaper while keeping the spectral-line intensity untouched, the CW is converted to an almost transformed-limited pulse train, as shown in Fig. 5(b). The spectral phase correction using the line-by-line pulse shaper is similar to dispersion-compensation experiments using a pulse shaper as a spectral phase equalizer [18]. The measured sampling scope traces (circles) have a full-width at half-maximum (FWHM) of 15 ps while the calculated transform-limited pulses (solid line) have a FWHM of 12 ps based on the spectrum shown in Fig. 3(b). The deviation between experiment and calculation is mainly due to the limited bandwidth of the 50-GHz photodiode. To show further evidence of nearly complete phase correction, the measured intensity autocorrelation of the generated pulses (17 ps, squares) and the calculated transform-limited pulse intensity autocorrelation (16.5 ps, solid line) are shown in Fig. 5(c). The excellent agreement between them demonstrates that the CW is converted to almost transform-limited pulses as short as 12 ps. All the spectral lines of the phase-modulated CW laser have 0 or π phase shift [8], making experimental implementation of phase correction simple. For a pure cosine driving waveform, the intensity/phase of spectral lines can be calculated analytically [9]. However, the driving waveform adapted from the clock signal of a BER test set in our experiment has strong higher harmonic components, which make it somewhat involved to accurately determine the phases of all spectral lines. To accurately predict the phase profile, the actual driving RF waveform (both its amplitude and shape) and V_π of the phase modulator must be known. In our experiment, the spectral phase profile of the modulated CW laser is first estimated by calculation assuming a pure cosine RF driving waveform (i.e., neglecting the harmonic distortion known to be present in our driving waveform), and then a conjugate spectral phase is applied and adjusted (change some spectral line phases between 0 and π) until the shortest pulses are obtained. In this experiment, the $+1$, $+3$, $+5$, $+6$, -6, and -7 order lines in Fig. 3(b) are controlled to have a π phase shift while the other lines have zero phase shift to compensate for the phases of the generated spectral lines. This simple procedure is sufficient for the purpose of the demonstration shown here. The accuracy of the spectral phase estimation by this procedure is also confirmed (at least for those dominant lines) by a spectral phase-measurement technique mentioned below. In addition to theoretically predicting the spectral phase profile using the information of RF driving waveform and V_π of the phase modulator, the spectral phase can be alternatively measured using other methods. Among the various optical techniques developed to characterize the spectral phase, an interferometry-based method [19], [20] is particularly appealing for the characterization of discrete spectral lines shown here, since this method also relies on spectral line-by-line control. Actually, we measured the phases of generated spectral lines using this method, which agree with the estimated spectral phases for those dominant spectral lines (from -5 to $+5$ order). The higher order spectral lines at edges have too little power to be accurately measured and have a negligible effect on this pulse generation experiment. Note that the pedestal in the generated pulses is mainly caused by the almost missing center spectral line (zeroth-order).

Previously, CW-to-pulse conversion was achieved by correcting spectral phase using single-mode fiber or other dispersion components [9]–[11]. However, only a simple spectral phase profile (such as quadratic) can be compensated in this way, making it difficult to achieve transform-limited pulses as successfully demonstrated here. Fiber Bragg gratings are able to compensate for complex spectral phases [22]–[24] but require relatively complicated design and have very limited tunability. Our demonstration also provides a simple approach to generate high-repetition-rate short pulses. In order to achieve shorter pulses comparable to those from high-repetition-rate mode-locked lasers, one just needs more spectral lines or broader optical bandwidth generated from the modulated CW, which can be fulfilled with technologies mentioned before.

E. Width- and Wavelength-Tunable Return-to-Zero (RZ) Pulse Generation

Rather than short-pulse generation, other waveforms or essential optical arbitrary waveform can be achieved with this approach since the intensity and phase of individual spectral lines can be manipulated. This is similar to our previous line-by-line pulse-shaping demonstration using a mode-locked laser [5]. Here, we show a simpler but still useful functionality.

Fig. 6 shows width- and wavelength-tunable RZ pulse generation, which we previously demonstrated using a mode-locked laser [21]. The pulse width is proportional to the inverse of the spectral bandwidth (after phase correction) or, roughly speaking, the number of the spectral lines. The spectra are controlled by the pulse shaper to have two lines [Fig. 6(a)], three lines [Fig. 6(b)], and four lines [Fig. 6(c); linear scale spectra are shown to compare the relative intensities of spectral lines]. The relative intensities between individual lines are controlled to make generated waveforms with negligible oscillation and pedestal. The corresponding pulse FWHMs are 55, 37, and 28 ps, respectively, agreeing well with the calculated waveforms. Specifically, for two spectral lines, the ideal waveform

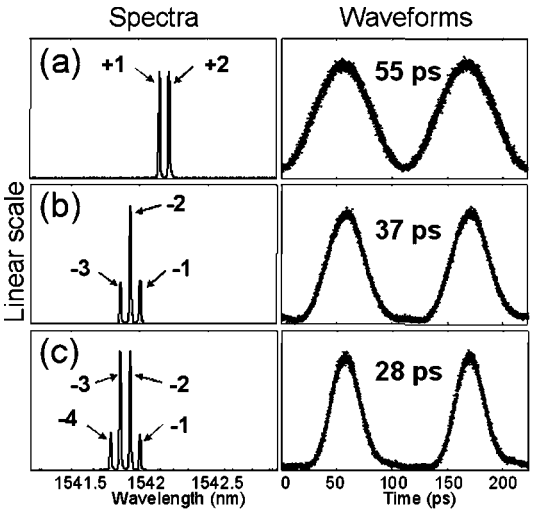

Fig. 6. Width- and wavelength-tunable RZ pulse generation. The spectra are controlled to have: (a) two lines, (b) three lines, and (c) four lines. The corresponding waveforms have width of 55, 37, and 28 ps. These pulses also have different and adjustable center wavelengths.

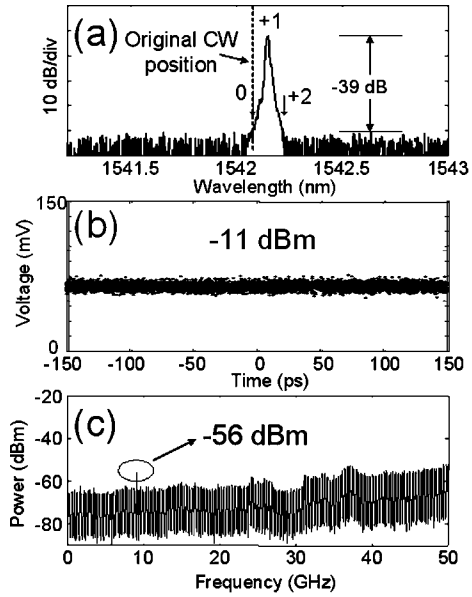

Fig. 7. Pulse-to-CW conversion and CW-to-CW wavelength conversion. (a) Optical spectrum of one filtered line, which is different from the input CW wavelength. (b) Corresponding CW waveform detected by a photodiode and (c) RF spectrum.

intensity profile in the time domain corresponds to a cosine function (with a dc offset). The waveform in Fig. 6(a) indeed demonstrates a 9.0-GHz cosine function. Together with the 12-ps pulses demonstrated in Fig. 5, a pulse-width tuning range of 12–55 ps at a 9.0-GHz repetition rate has been shown. Pulses in Fig. 6 also have different but adjustable center wavelengths, demonstrating a wavelength-tunability function. Larger wavelength tuning range can be readily achieved by tuning the CW center wavelength. Width- and wavelength-tunable pulses are widely used in optical fiber communication systems and optical networks, including RZ format transmission, soliton systems, optical time-division multiplexing, optical code-division multiple-access, and optical packet generation [21].

F. Single-Line Filtering (Pulse-to-CW Conversion and Wavelength Conversion)

In general, waveform fidelity after pulse shaping depends on the precision with which the frequency spectrum can be controlled. In order to gain insight into pulse-shaper requirements in the line-by-line regime, here we examine what is perhaps the simplest and most fundamental operation in line-by-line shaping: selection of a single spectral line, converting an input frequency comb into a CW field. Our results show the critical importance of achieving very high suppression of unwanted lines.

Fig. 7(a) shows the use of the line-by-line shaper to filter out one single spectral line, which is different from the input CW wavelength. The undesired lines are almost completely suppressed (which is higher than 39 dB) and are buried in the noise background. In this single-line filtering experiment, slits are used to assist suppressing undesired lines. Fig. 7(b) and (c) shows the corresponding CW waveform detected by a photodiode and its RF spectrum. According to Fig. 7(b) and (c), there is a 45-dB contrast ratio between dc and the first harmonic in the RF spectrum. According to our later discussion, this suggests the suppression ratio of unwanted lines in the optical spectrum is as large as 48–54 dB. Comparing with the pulse-generation data demonstrated in Figs. 5 and 6, this demonstrates the pulse-to-CW conversion function. If data are modulated onto the pulses, this conversion essentially accomplishes RZ-to-non-return-to-zero (NRZ) format conversion as previously demonstrated using a mode-locked laser [21]. Further, the input CW and filtered output CW have different wavelength, which demonstrates CW-to-CW wavelength conversion. Wavelength conversion based on this scheme also works if data are modulated on the input CW. Previously such wavelength conversion was achieved using an arrayed waveguide grating [12]. However, multiple lines were typically produced instead of a single output line (pure CW) due to limited spectral suppression. The almost pure CW wavelength conversion demonstrated here may be useful to reduce crosstalk in wavelength conversion for application to dense wavelength-division-multiplexing systems.

G. Correlation Between Optical Spectra and Waveforms

The good quality CW waveform in Fig. 7(b) is possible only because very high suppression of unwanted optical lines can be achieved. Even very slightly unsuppressed lines may introduce significant distortions, as shown in Fig. 8. Here, two spectral lines are selected, and one of them is intensity controlled with variable suppression ratio from −39 dB (shown in Fig. 7) to 0 dB. As little as a −29-dB lower unsuppressed spectral line distorts the "CW" waveforms visibly, in which the dots are measured results from the sampling scope and the solid curves are calculations based on two spectral lines (e.g., one desired and one partially suppressed). On the other hand, when the ratios of the two spectral lines approach 0 dB, the waveform changes are relatively small. The calculations and measurements (average of 20 times sampling scope traces) agree well with each other. The minima of the measured waveforms are higher than calculations, which is likely caused by the noise from the optical

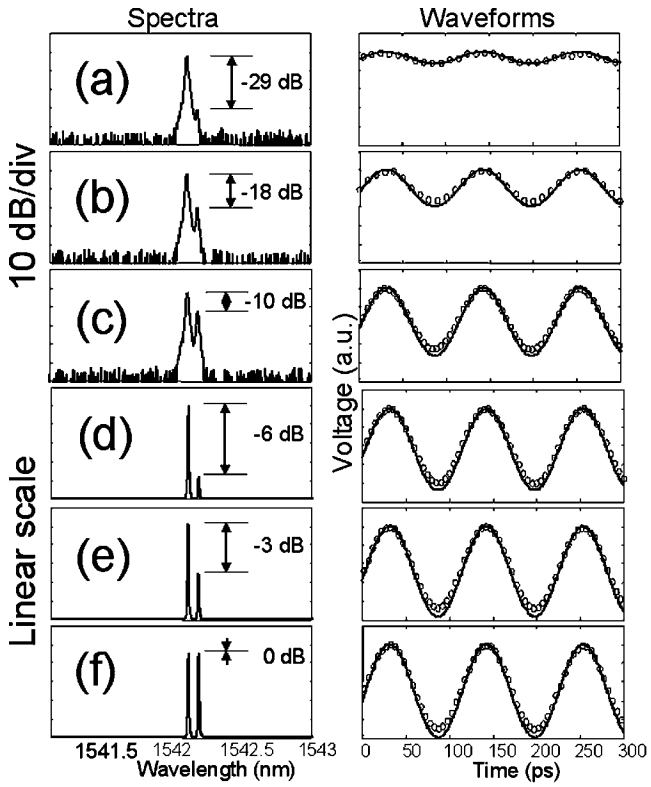

Fig. 8. Effects of suppression ratio on the waveforms. The suppression ratios are (a) −29 dB, (b) −18 dB, (c) −10 dB, (d) −6 dB, (e) −3 dB, and (f) 0 dB. Circles in the waveforms are measured data while the lines are calculated ideal cosine waveforms. Spectra in (a)–(c) are log scale and spectra in (d)–(f) are linear scale.

amplifier because the incoherent noise increases the background level of the waveforms.

To understand these results, consider the field of two lines in the frequency domain, which can be expressed as

$$M(\tilde{f}) = \delta(\tilde{f}) + \sqrt{\beta} \cdot \delta(\tilde{f} - \Delta f) \cdot \exp(-j\theta) \qquad (1)$$

where $\delta(\cdot)$ represents the impulse function, β and θ represent the relative intensity and phase between the two spectral lines, and Δf is the frequency spacing between two lines. The baseband frequency $\tilde{f} = f - f_0$, where f is optical frequency of spectral line and f_0 is some carrier frequency. In the time domain, the intensity profile can be obtained by Fourier transform as

$$|m(t)|^2 = 1 + \beta + 2\sqrt{\beta} \cdot \cos(2\pi\Delta f t - \theta)). \qquad (2)$$

It is a cosine waveform with dc offset as expected. The ratio between the peak-to-peak and mean value of the waveform is $4\sqrt{\beta}/(1+\beta)$, as shown in Fig. 9. When β is small, the ratio is proportional to $4\sqrt{\beta}$, which suggests that a single −20-dB unsuppressed line will cause ∼40% variation on the waveform. When β is close to 0 dB, this ratio becomes saturated. The above analysis satisfactorily explains the results in Fig. 8.

The key point is that extremely strong suppression of adjacent lines is required to extract a time-independent CW field from the mode-locked comb. This, in turn, suggests the need for pulse-shaper spectral resolution much more than the spectral

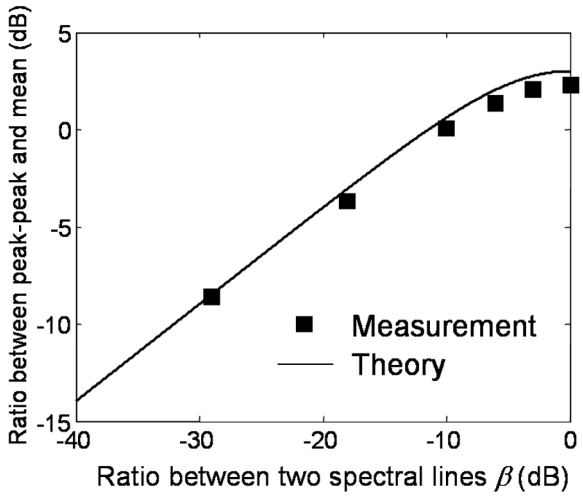

Fig. 9. Correlation between optical spectra and waveforms for two spectral lines.

line spacing. Similar considerations are likely to prove at least equally important in line-by-line pulse shaping for the generation of more complex waveforms made up of a multiplicity of lines.

H. Correlation Between Optical Spectra and RF Spectra

In the single spectral line-filtering experiment shown in Fig. 7, the unsuppressed line is buried in the noise background of optical spectrum. A more sensitive approach to monitor the suppression ratio is to measure the RF spectrum after O/E conversion. By comparing the dc and the first harmonic of the RF spectrum, further information about the optical spectrum (such as the suppression ratio) can be deduced. This prompts us to investigate the correlation between optical spectra and RF spectra. For experimental convenience, the first and second harmonics in the RF spectrum are compared, but the principle can be applied to all other harmonics and to dc.

Fig. 10(a) shows a set of three selected spectral lines with identical spectral phases and the corresponding calculated and measured RF spectra (single-sided power spectra). The relative intensities of these three lines are not intentionally controlled but rather are set arbitrarily to show the general correlation between optical and RF spectra. These three lines have identical phases directly after phase-modulated CW (i.e., no additional spectral phase applied from the LCM). Since there are three spectral lines, only dc and the first and second harmonics appear in the RF spectrum. The RF spectrum can be calculated based on the intensity and phase information of the optical spectrum by the procedure shown in (3), at the bottom of the following page, where $A(f)$ is the optical spectrum, $\Phi(f)$ is optical spectral phase, $i(t)$ is the signal after O/E conversion, $I(\tilde{f})$ is the Fourier transform of $i(t)$, and $|I(\tilde{f})|^2$ is the RF power spectrum. In our calculation, the spectral line intensities are measured values from OSA, and the three selected spectral lines have identical spectral phases directly after the phase-modulated CW. The agreement between calculation and measurement is good. The small discrepancies are mainly caused by the ∼1-dB variations in the frequency response of the photodiode (which

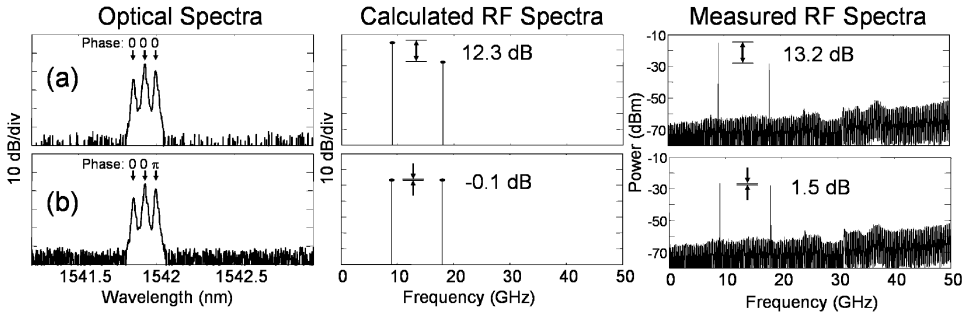

Fig. 10. Correlation between optical spectra and RF spectra for three spectral lines. (a) Three lines with identical phases. (b) Three lines with one line π-phase-shifted.

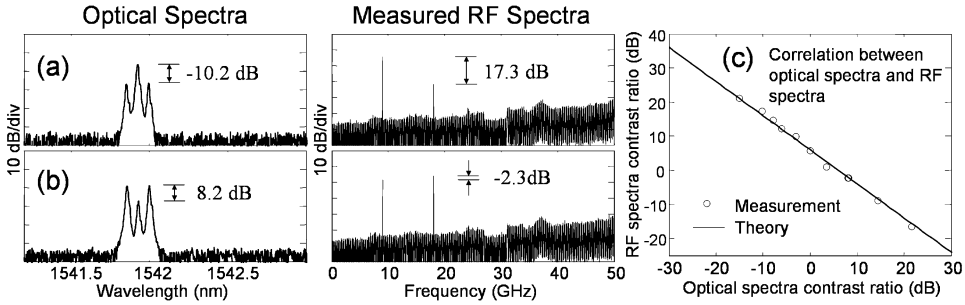

Fig. 11. Correlation between optical spectra and RF spectra for three spectral lines with identical phases, where the two outside lines are controlled to have equal intensity. (a) The center line is higher than the outside lines. (b) The center line is lower than the outside lines. (c) RF spectra contrast ratio versus optical spectra contrast ratio.

are not considered) and the possible contributions from imperfect suppression ratio for spectral lines other than those three selected. Fig. 10(b) shows the results for three lines with similar intensities but one line π–phase-shifted under LCM control. The RF spectrum changes significantly, and the first and second harmonics have almost equal powers. Again, agreement with calculations is good. This shows the possibility to synthesize the RF spectrum by line-by-line pulse shaping on the intensity and phase of optical spectrum.

If we still select three lines but control the outside two lines to have equal intensity, we have the results shown in Fig. 11(a), with the center line higher than the outside lines and, in Fig. 11(b). with the center line lower than the outside lines. To simplify the study, we only focus on the case in which these three lines have identical phases. Assuming that the ratio of the optical power spectral density between each of the outside lines and the center line is r, the field of three lines with identical phases can be expressed as

$$A(\tilde{f}) = \delta(\tilde{f}) + \sqrt{r}\cdot\delta(\tilde{f}-\Delta f) + \sqrt{r}\cdot\delta(\tilde{f}+\Delta f). \quad (4)$$

After simple calculation using the procedure shown in (3), the ratio of RF spectrum between the first and second harmonics is $4/r$. This relationship is confirmed as shown in Fig. 11(c) by scanning the ratio of optical spectral line intensities (r) by programming the pulse shaper for intensity control. Note that, since only ratios (or relative intensities) are measured in Fig. 11(c), no adjustable parameters are needed in the theory to fit the measurements.

Similarly, the ratio of RF spectrum between dc and first harmonic can be calculated as $(1+2r)^2/(8r)$, which reduces to $1/(8r)$ when the outside lines are weak. Based on this analysis, the 45-dB contrast ratio between dc and the first harmonic of RF spectrum in Fig. 7 suggests as much as a 54-dB suppression ratio in the optical spectrum assuming there are two equal unsuppressed lines with the same phase around the single desired line. Note that, in Fig. 7, the center line has a π phase shift relative to the two outside lines (which are not seen because they are buried in the noise), but the conclusion drawn here does not change. Alternatively, if there is only one strong unsuppressed line in Fig. 7, as described by (1), the ratio of the RF spectrum between dc and first harmonic can be calculated as $(1+\beta)^2/(2\beta)$, which reduces to $1/(2\beta)$ when the single unsuppressed line is small. Under this assumption, the 45-dB contrast ratio between dc and the first harmonic of the RF spectrum in Fig. 7 suggests as much as a 48-dB suppression ratio in the optical spectrum assuming that there is only one strong unsuppressed line.

$$|A(f)|^2 \xrightarrow{\surd} |A(f)| \xrightarrow{Phase} A(f)e^{i\Phi(f)} \xrightarrow{IFFT} a(t) \xrightarrow{||^2} i(t) \xrightarrow{FFT} I(\tilde{f}) \xrightarrow{||^2} \left|I(\tilde{f})\right|^2 \quad (3)$$

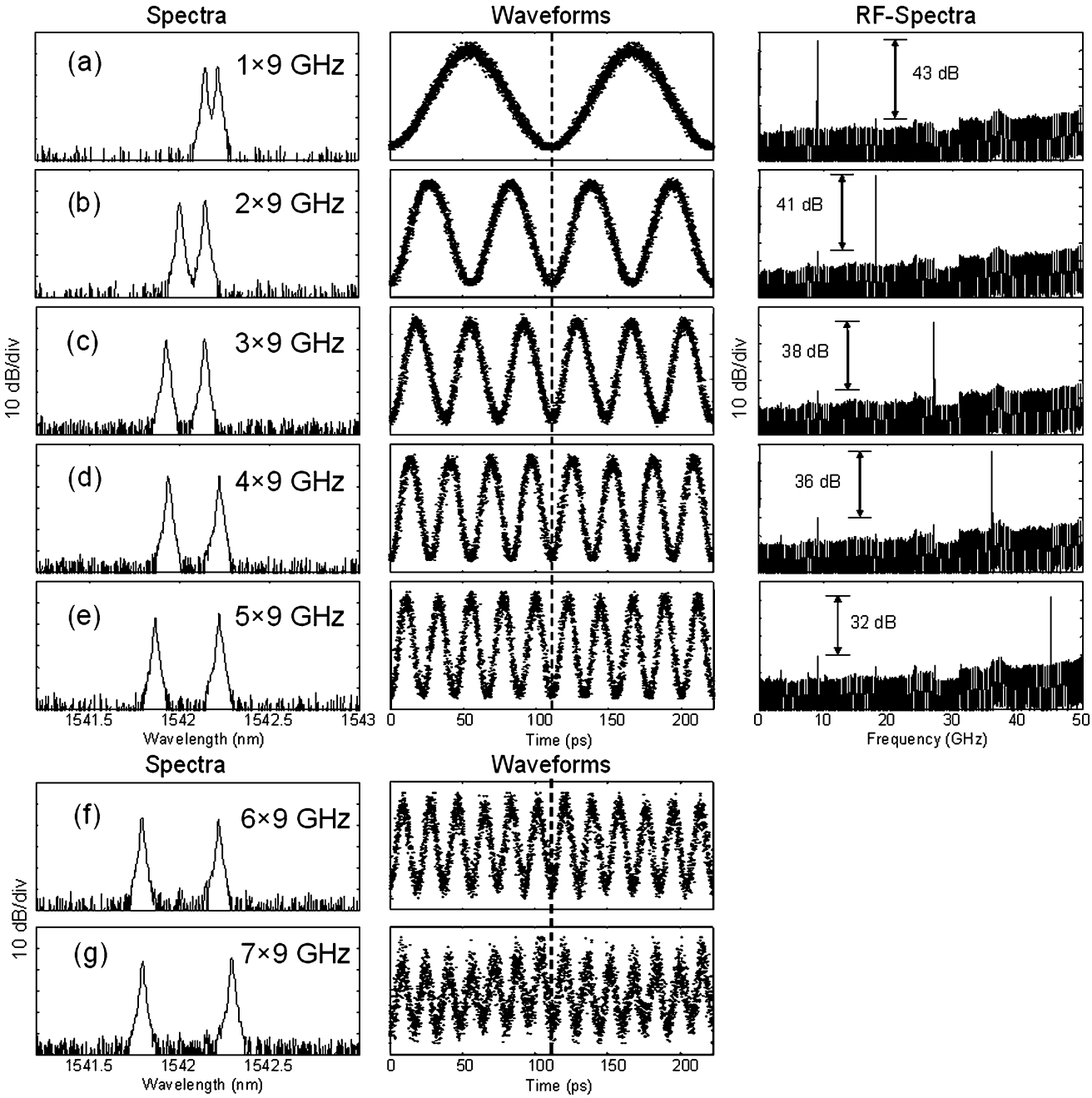

Fig. 12. Two selected spectral lines are controlled to be separated by: (a) 1 × 9 GHz, (b) 2 × 9 GHz, (c) 3 × 9 GHz, (d) 4 × 9 GHz, (e) 5 × 9 GHz, (f) 6 × 9 GHz, and (g) 7 × 9 GHz. The corresponding microwave signals are generated after O/E conversion using a 50-GHz photodiode. RF spectra are measured for (a)–(e) to show the harmonics suppression.

I. Microwave Waveform Synthesis

Here, we select two lines with different separations to beat for microwave waveform synthesis, as shown in Fig. 12. The waveforms are generated after optoelectro conversion using a 50-GHz photodiode, where 9-, 18-, 27-, 36-, 45-, 54-, and 63-GHz waveforms are shown. The undesired spectral lines are well suppressed (e.g., higher than 34-dB suppression ratio, limited by the noise floor of the optical spectra measurements), making high-purity microwave generation possible. The RF spectra measurements (up to 45-GHz waveform) show the harmonic suppression from 43 to 32 dB, depending on the frequencies of waveforms. Using a similar procedure as in Section II-H and (3), the optical spectra suppression ratio can be estimated from the harmonic suppression of the RF spectrum, under certain assumptions. For example, in Fig. 12(a), assuming that there are two equal unsuppressed lines around the two equal selected lines and that all of them have identical phases, the 43-dB RF harmonic suppression ratio suggests 52-dB suppression ratio in the optical spectrum. Note that other assumptions (for example, unequal unsuppressed lines or nonidentical phases) will yield somewhat different estimates.

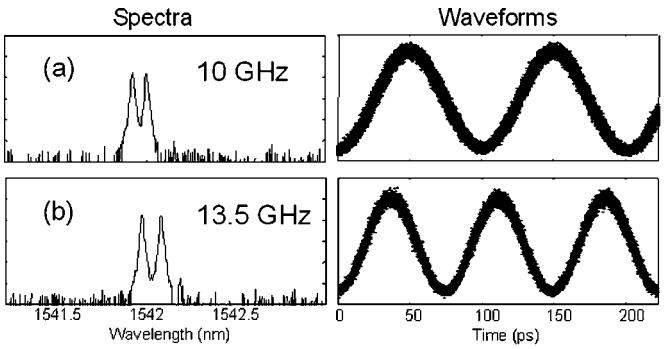

Fig. 13. Two selected spectral lines are separated by (a) 10 GHz and (b) 13.5 GHz by changing the RF driving frequencies accordingly.

The noise of the waveforms increases with the frequency of synthesized waveforms. This can be explained by noting that two selected lines with larger separation have smaller powers and thus suffer from more noise from optical amplifier.

Only 9 GHz and its harmonics waveforms are synthesized in Fig. 12. Other frequencies and their harmonics can be readily generated by tuning the driving frequency to the modulator. For example, Fig. 13 shows two waveforms at 10.0 and 13.5 GHz by driving the phase modulator appropriately and selecting two lines. In this way, almost any frequency supported by the bandwidth of the generated spectral lines can be synthesized using RF driving electronics tunable only over a relatively narrow range about ~ 10 GHz. Optically generated microwave signals have the potential to impact fields such as ultra-wideband (UWB) wireless communications, impulsive radar, and radio-over-fiber.

III. Conclusion

We have demonstrated optical processing based on spectral line-by-line pulse shaping on a phase-modulated CW laser. We have shown various processing functions including CW-to-pulse conversion, width- and wavelength-tunable RZ pulse generation, pulse-to-CW conversion, wavelength conversion, and microwave signal generation. We also quantitatively studied the correlations between optical spectra, time-domain waveforms, and RF spectra. These studies clearly reveal the critical need for very high suppression of unwanted frequencies in line-by-line shaping. Phase modulation of a CW source provides a simple but very flexible approach to generate spectral lines with reasonably good stability for line-by-line pulse shaping.

Acknowledgment

The authors would like to acknowledge R. Huang for his help in the experiment.

References

[1] A. M. Weiner, "Femtosecond pulse shaping using spatial light modulators," *Rev. Sci. Instr.*, vol. 71, no. 5, pp. 1929–1960, May 2000.

[2] Z. Jiang, D. S. Seo, D. E. Leaird, and A. M. Weiner, "Spectral line-by-line pulse shaping," *Opt. Lett.*, vol. 30, no. 12, pp. 1557–1559, Jun. 2005.

[3] T. Yilmaz, C. M. DePriest, T. Turpin, J. H. Abeles, and P. J. Delfyett, "Toward a photonic arbitrary waveform generator using a modelocked external cavity semiconductor laser," *IEEE Photon. Technol. Lett.*, vol. 14, no. 11, pp. 1608–1610, Nov. 2002.

[4] S. Etemad, T. Banwell, S. Galli, J. Jackel, R. Menendez, P. Toliver, J. Young, P. Delfyett, C. Price, and T. Turpin, "Optical-CDMA incorporating phase coding of coherent frequency bins: Concept, simulation, experiment," in *Proc. Optical Fiber Conf.*, Los Angeles, CA, 2004, p. FG5.

[5] Z. Jiang, D. E. Leaird, and A. M. Weiner, "Line-by-line pulse shaping control for optical arbitrary waveform generation," *Opt. Express*, vol. 13, no. 25, pp. 10431–10439, Dec. 2005.

[6] T. Kobayashi, T. Sueta, Y. Matsuo, and Y. Cho, "High-repetition-rate optical pulse-generator using a Fabry-Perot electrooptic modulator," *Appl. Phys. Lett.*, vol. 21, no. 8, pp. 341–343, Oct. 1972.

[7] M. Kourogi, T. Enami, and M. Ohtsu, "A coupled-cavity monolithic optical frequency comb generator," *IEEE Photon. Technol. Lett.*, vol. 8, no. 12, pp. 1698–1700, Dec. 1996.

[8] S. Hisatake, Y. Nakase, K. Shibuya, and T. Kobayashi, "Generation of flat power-envelope terahertz-wide modulation sidebands from a continuous-wave laser based on an external electro-optic phase modulator," *Opt. Lett.*, vol. 30, pp. 777–779, Apr. 2005.

[9] T. Kobayashi, H. Yao, K. Amano, Y. Fukushima, A. Morimoto, and T. Sueta, "Optical pulse compression using high-frequency electrooptic phase modulation," *IEEE J. Quantum Electron.*, vol. 24, no. 2, pp. 382–387, Feb. 1988.

[10] H. Murata, A. Morimoto, T. Kobayashi, and S. Yamamoto, "Optical pulse generation by electrooptic-modulation method and its application to integrated ultrashort pulse generators," *IEEE J. Sel. Topics Quantum Electron.*, vol. 6, no. 6, pp. 1325–1331, Nov./Dec. 2000.

[11] J. van Howe, J. Hansryd, and C. Xu, "Multiwavelength pulse generator using time-lens compression," *Opt. Lett.*, vol. 29, no. 13, pp. 1470–1472, Jul. 2004.

[12] E. Yamada, H. Sanjoh, M. Ishikawa, and Y. Yoshikuni, "High-speed wavelength switching in wavelength conversion using spectral duplication," in *Proc. Opt. Fiber Conf.*, Atlanta, GA, 2003, p. MF93.

[13] G. Qi, J. Yao, J. Seregelyi, S. Paquet, and C. Belisle, "Optical generation and distribution of continuously tunable millimeter-wave signals using an optical phase modulator," *J. Lightwave Technol.*, vol. 23, no. 9, pp. 2687–2695, Sep. 2005.

[14] S. T. Cundiff, "Phase stabilization of ultrashort optical pulses," *J. Phys. D*, vol. 35, no. 8, pp. R43–R59, Apr. 2002.

[15] S. Gee, F. Quinlan, S. Ozharar, and P. J. Delfyett, "Simultaneous optical comb frequency stabilization and super-mode noise suppression of harmonically mode-locked semiconductor ring laser using an intracavity etalon," *IEEE Photon. Technol. Lett.*, vol. 17, no. 1, pp. 199–201, Jan. 2005.

[16] D. J. Jones, S. A. Diddams, J. K. Ranka, A. Stentz, R. S. Windeler, J. L. Hall, and S. T. Cundiff, "Carrier-envelope phase control of femtosecond mode-locked lasers and direct optical frequency synthesis," *Science*, vol. 288, pp. 635–639, Apr. 2000.

[17] T. Udem, R. Holzwarth, and T. W. Hansch, "Optical frequency metrology," *Nature*, vol. 416, pp. 233–237, Mar. 2002.

[18] Z. Jiang, S.-D. Yang, D. E. Leaird, and A. M. Weiner, "Fully dispersion compensated ~ 500 fs pulse transmission over 50 km single mode fiber," *Opt. Lett.*, vol. 30, no. 12, pp. 1449–1451, Jun. 2005.

[19] P. Kockaert, M. Peeters, S. Coen, P. Emplit, M. Haelterman, and O. Deparis, "Simple amplitude and phase measuring technique for ultra-high-repetition-rate lasers," *IEEE Photon. Technol. Lett.*, vol. 12, no. 2, pp. 187–189, Feb. 2000.

[20] Z. Jiang, D. E. Leaird, and A. M. Weiner, "Optical arbitrary waveform generation and characterization using spectral line-by-line control," *J. Lightwave Technol.*, to be published.

[21] ——, "Width and wavelength tunable optical RZ pulse generation and RZ-to-NRZ format conversion at 10 GHz using spectral line-by-line control," *IEEE Photon. Technol. Lett.*, vol. 17, no. 12, pp. 2733–2735, Dec. 2005.

[22] P. Petropoulos, M. Ibsen, A. D. Ellis, and D. J. Richardson, "Rectangular pulse generation based on pulse reshaping using a superstructured fiber Bragg grating," *J. Lightwave Technol.*, vol. 19, no. 5, pp. 746–752, May 2001.

[23] M. Marano, S. Longhi, P. Laporta, M. Belmonte, and B. Agogliati, "All-optical square-pulse generation and multiplication at 1.5 mm by use of a novel class of fiber Bragg gratings," *Opt. Lett.*, vol. 26, no. 20, pp. 1615–1617, Oct. 2001.

[24] N. K. Berger, B. Levit, A. Bekker, and B. Fischer, "Reshaping periodic light pulses by pulse multiplication," in *Proc. Conf. Lasers and Electro-Optics*, Baltimore, MD, 2005, p. JWB54.

Zhi Jiang (S'03) received the B.S. (highest Honors) and M.S. degrees from the Department of Electronics Engineering, Tsinghua University, Beijing, China, in 1999 and 2002, respectively. He is currently working toward the Ph.D. degree at the School of Electrical and Computer Engineering, Purdue University, West Lafayette, IN.

His research focuses on the areas of ultrafast technology, optical pulse shaping, optical fiber communication, fiber nonlinearity.

Mr. Jiang received the Ross and Mary I. Williams Fellowship, Purdue University, in 2002–2003. He was selected as a finalist for the 2005 OSA New Focus/Bookham Student Award, and he is one of the recipients of the 2005 IEEE/LEOS Graduate Student Fellowships.

Daniel E. Leaird (M'01–SM'05) was born in Muncie, IN, in 1964. He received the B.S. degree in physics from Ball State University, Muncie, IN, in 1987, and the M.S. and Ph.D. degrees from the School of Electrical and Computer Engineering, Purdue University, West Lafayette, IN, in 1996 and 2000 respectively.

He joined Bell Communications Research (Bellcore), Red Bank, NJ, as a Senior Staff Technologist in 1987 and later advanced to Member of Technical Staff. From 1987 to 1994, he was with the Ultrafast Optics and Optical Signal Processing Research Group, where he was a key team member in research projects in ultrafast optics, such as shaping of short optical pulses using liquid-crystal modulator arrays, investigation of dark soliton propagation in optical fibers, impulsive stimulated Raman scattering in molecular crystals, and all-optical switching. He is currently a Senior Research Scientist and Laboratory Manager of the Ultrafast Optics and Optical Fiber Communications Laboratory, School of Electrical and Computer Engineering, Purdue University, where he has been since 1994. He has coauthored approximately 60 journal articles and 80 conference proceedings and holds two U.S. patents. He also serves as a frequent reviewer for *Optics Letters*, *Optics Express*, IEEE PHOTONICS TECHNOLOGY LETTERS, *Applied Optics*, and *Journal of the Optical Society of America B*.

Dr. Leaird was the recipient of several awards for his work in the ultrafast optics field, including a Bellcore "Award of Excellence," a Magoon Award for outstanding teaching, and an Optical Society of America/New Focus Student Award. He is active in the optics community and professional organizations including the Optical Society of America and the IEEE Lasers and Electro-Optics Society, where he is a member of the Ultrafast Technical Committee as well as serving as a consultant to venture capitalists by performing technical due diligence, in addition to serving on National Science Foundation review panels in the SBIR program.

Andrew M. Weiner (S'84–M'84–SM'91–F'95) received the Sc.D. degree in electrical engineering from the Massachussets Institute of Technology (MIT), Cambridge, in 1984.

From 1979 to 1984, he was a Fannie and John Hertz Foundation Graduate Fellow at MIT. In 1984, he joined Bellcore, first as a Member of Technical Staff and later as a Manager of Ultrafast Optics and Optical Signal Processing Research. He joined Purdue University, West Lafayette, IN, in 1992 and is currently the Scifres Distinguished Professor of Electrical and Computer Engineering. From 1997 to 2003, he served as the ECE Director of Graduate Admissions. His research focuses on ultrafast optical signal processing and high-speed optical communications. He is especially well known for pioneering the field of femtosecond pulse shaping, which enables generation of nearly arbitrary ultrafast optical waveforms according to user specification. He has published five book chapters and over 175 journal articles. He has been the author or coauthor of over 300 conference papers, including approximately 80 conference-invited talks, and has presented over 70 additional invited seminars at universities or industries. He holds eight U.S. patents.

Prof. Weiner is a Fellow of the Optical Society of America. He has been the recipient of numerous awards for his research, including the Hertz Foundation Doctoral Thesis Prize (1984), the Adolph Lomb Medal of the Optical Society of America (1990), awarded for pioneering contributions to the field of optics made before the age of 30, the Curtis McGraw Research Award of the American Society of Engineering Education (1997), the International Commission on Optics Prize (1997), the IEEE LEOS William Streifer Scientific Achievement Award (1999), the Alexander von Humboldt Foundation Research Award for Senior U.S. Scientists (2000), and the inaugural Research Excellence Award from the School of Engineering at Purdue University (2003). He has served as Co-Chair of the Conference on Lasers and Electrooptics and the International Conference on Ultrafast Phenomena and associate editor of several journals. He has also served as Secretary/Treasurer of IEEE LEOS and as a Vice-President of the International Commission on Optics (ICO).